

Estimation of the distribution of reactivity for powdered cellulose pyrolysis in isothermal experimental conditions using the Bayesian inference

Bojan Janković

Received: 17 November 2014 / Accepted: 9 May 2015 / Published online: 14 May 2015
© Springer Science+Business Media Dordrecht 2015

Abstract Bayesian inference was used to test the powdered cellulose pyrolysis, under the isothermal experimental conditions. A completely new procedure that was based on obtaining the reliable distribution functions of the effective (apparent) activation energy (E_a) values by the statistical derivation of prior and posterior functions was introduced. It has been found that the pyrolysis of the powdered cellulose can be described by the kinetics, which differs from the first-order model. It was established that the apparent activation energy value presented as average magnitude in the conversion fraction range of $0.20 \leq \alpha \leq 0.65$ does not represent the “lumped” kinetic parameter, so in indicated conversion range, the pyrolysis process can be described through single-step reaction model with six-eighths-order ($n^* = 0.75$) kinetics. Based on the presented Bayesian inference results, it was assumed that mechanism of pyrolysis takes place through the decomposition reactions which start from the cellulose chains. From the main characteristics of the prior distribution, relationship between the ingredients of Bayesian inference and the cellulose characteristic energy constant (c) [which is related to the rigidity angle (ψ) as a measure of tenseness of the cellulose chains]

has been established in this paper. Based on evaluated prior and posterior distributions and their characteristics, it was found that the pyrolysis process of powdered cellulose takes place probably through formation of levoglucosan, where depolymerization represents the primary reaction path. Bayesian approach can be applied to highly structured reaction systems and complex physico-chemical processes, which include the reactivity distribution of various energy counterparts, which has been often un-tractable by traditional statistical access.

Keywords Cellulose · Isothermal pyrolysis · Non-integer kinetics · Bayesian inference · Posterior distribution

Introduction

Cellulose is the most abundant natural polymer and becomes part of all plants. This biopolymer in the plant world, only in the cotton fibers occurs in almost pure form. Native cellulose is a product of photosynthesis, which takes place in plants by two low-energy potential substances, CO_2 and H_2O , under the influence of electromagnetic radiation of the sun, when a substance of high chemical potential occurs. It is believed that in this process, the enzyme systems participate (which can be found in the cell walls) whereby the glycoprotein molecules are primary.

B. Janković (✉)
Faculty of Physical Chemistry, Department for Dynamics and Matter Structure, University of Belgrade, Studentski trg 12-16, P. O. Box 137, 11001 Belgrade, Serbia
e-mail: bojanjan@ffh.bg.ac.rs

Cellulose is the first polymer on which the structural organizations were studied (Jovanović 1989). Cellulose makes about 40–50 % of the dry weight of the wood. It is a polysaccharide composed of molecules with β -D-glucopyranose linked by (1,4)-glycosidic connections. Cellulose molecules are linear, while the degree of polymerization varies from one to the other raw materials.

Studying the cellulose pyrolysis is significant in terms of better understanding of mechanism of the process related to biomass systems and application of biomass in obtaining the fuels and chemicals.

On-line pyrolysis is directly correlated to the solid mass loss versus temperature or time and kinetic models, usually applying isothermal and dynamic (non-isothermal) thermogravimetric analysis (TGA) coupled with or without Fourier transformation infrared spectrometry (FTIR) or mass spectrometry (MS). On the other hand, off-line pyrolysis refers to carrying out the yield of main products [such as gases, liquids and solids (bio-chars)], variation of the compositions in gaseous or liquid products influenced by intrinsic characteristics and experimental conditions, in order to improve the pyrolysis process optimization for the energy or chemicals productions.

The current work is linked to the use of on-line pyrolysis of powder cellulose samples (as an «isolated» reaction system), conducted through the implementation of the thermogravimetry (TG). Bearing in mind that dry biomass fuels are comprised of about 50 % cellulose by weight, the study of pyrolysis kinetics of cellulose is essential to the chemical design of biomass pyrolysis.

A large number of researchers have studied the cellulose pyrolysis kinetics. The power law kinetic equation with a reaction order of one has been adopted as the reaction model function of cellulose pyrolysis without confirmation (Agrawal 1988a, b; Antal and Varhegyi 1995; Bigger et al. 1998; Blasi 1994; Bradbury et al. 1979; Conesa et al. 1995; Diebold 1994; Grønli et al. 1999; Varhegyi and Antal 1989). In the similar type of paper (Eom et al. 2006), we could check whether or not the first-order reaction would be proper to represent the cellulose pyrolysis kinetics. In the current case, the reaction order was estimated to be about 1.50, without constraint on the reaction order. Also, the disparities of the kinetic parameters were apparent. Owing to correlation among the kinetic parameters, fixation of reaction order forces the kinetic

parameters to deviate from the real ones. Also, the differences in apparent activation energy (E_a) values between model-fitting and model-free kinetic methods (Vyazovkin and Wight 1999) were noted (Liu et al. 2013; Cabrales and Abidi 2010; Arora et al. 2011; Poletto et al. 2012). Likewise, the disagreements regarding to reaction mechanisms were also found (Liao et al. 2004; Mettler et al. 2012; Capart et al. 2004; Sánchez-Jiménez et al. 2011, 2013; Emsley and Stevens 1994; Ding and Wang 2008). Because of all above-mentioned, it is essential to derive the exact or correct form of the reaction model for cellulose pyrolysis, where the investigated samples are present in the powder form.

In this paper, the results obtained by kinetic analysis based on isothermal thermogravimetric data were compared with a new approach, which involves the estimation of the distribution of reactivity assuming the distribution of the apparent (effective) activation energy values in the complex pyrolysis process of the powdered cellulose, and which represents the intrinsic (associated and inseparable) characteristic of the structural changes of cellulose during the pyrolysis. The current distribution has been carried out using the Bayesian inference approach.

Decision theory as the name suggests, deals with the problem of making decisions. The statistical decision theory deals with making decisions using the knowledge of mathematical statistics.

Classical statistics uses information from the observed statistical sample for the purpose of determining the value of the unknown parameter, θ . On the other hand, the decision theory combines information obtained from the observed statistical sample with various relevant aspects of the problem in order to make the best decisions. Two common aspects of the problem which, in decision theory are further discussed represent the following items: *i*) the possible consequences of decisions and *ii*) a priori information. Unknown θ value that affects the decision-making process is called *state*. The set of all states is marked with Ω . When information about θ is obtained through the experiments, it is common that they are planning in the sense that designation has distribution which is attributed to an unknown parameter. Then θ is called the parameter, and Ω is the parameter space.

Bayesian analysis is a combination of a priori information [marked by $\pi(\theta)$] and information from the observed statistical sample (usually marked by

“ x ”) to obtain the posterior distribution for a given “ x ”, based on which the decisions and conclusions are made.

It should be mentioned that Bayesian methods allow incorporation of the scientific hypothesis in current analysis (by means of prior distribution) and can be applied to problems whose structure is too complex for conventional statistical methods. Thus, one of the serious problems that it is worth to consider by applying the Bayesian statistical methods is the cellulose pyrolysis, which represents the complex physico-chemical process, consisting of the entire set of decomposition reactions, which originate from the basic molecules. Our goal is to get the reliable distribution functions of effective (apparent) activation energy (E_a) values by the statistical derivation of prior and posterior functions (Martz and Waller 1985; Robert 2001; Lee 2012). For this purpose, it was exploited the most frequently used distribution from the conventional statistical analysis, and its selection is based on the statistical characteristics of the experimental distribution of E_a values.

A central element of this paper is the specification of a probability model which is assumed to describe the cellulose pyrolysis reaction mechanism, which has generated the observed data (marked by “ D ”) ψ as a function of a (possibly multidimensional) parameter space Ω . All conclusions were statistically conditioned by characteristics of assumed probability model for the investigated cellulose pyrolysis process.

Experimental

Material

The material studied was cellulose powder (Sigma-Aldrich) with a particle size of 50 μm . The cellulose powder samples were directly used for thermogravimetric (TG) measurements under isothermal conditions, at various operating temperatures. In this paper, the ultimate analysis was carried out which gives us the actual chemical composition of the used samples. The results of this analysis are expressed as dry ash free basis (dafb). The corresponding analysis was performed according to the recommendations of current standards (Milne et al. 1990). Results of the ultimate analysis were as follows: C = 43.65 %, H = 6.57 %, O = 49.68 % and N = 0.10 % [dafb]. The current

O/C and H/C ratios (through percent relationships) were found as: 1.14 and 0.15, respectively.

Thermo-analytical (TA) measurements

The isothermal (static) investigations were carried out on a thermogravimetric (TG) analyzer (TA Instruments SDT 2960, TA Instruments, 159 Lukens Drive, New Castle, UK, DE 19720) device capable of the simultaneous thermal analysis measurements. For all cellulose samples, the value of the heating rate used to achieve the desired operating temperature was $\beta = 100 \text{ }^\circ\text{C min}^{-1}$. All thermogravimetric experiments were carried out in the atmosphere of the flowing nitrogen (flow rate of $\varphi = 50 \text{ mL min}^{-1}$). The powder samples (towards the particle sizes of 50 μm) with the initial mass of 6–8 mg were taken in an open platinum crucible, where the crucible weight was calibrated to zero. The isothermal thermogravimetric (TG) measurements were carried out at the four different operating temperatures [$T_i = 300, 320, 330$ and $340 \text{ }^\circ\text{C}$ ($i = 4$)]. All measurements were repeated at these operating temperatures until the consistency of the experimental data that has been identified.

Theoretical background

Isoconversional (“model-free”) methods

The concepts of solid-state kinetics were established (Hedwall 1938) on the basis of experiments carried out under isothermal conditions. This was long before the first instruments for non-isothermal measurements became commercially available. The governing kinetic equation:

$$\frac{d\alpha}{dt} = A \cdot \exp\left(-\frac{E_a}{RT}\right) \cdot f(\alpha), \quad (1)$$

where t is the time [min], A is the pre-exponential factor [min^{-1}], E_a is the apparent activation energy ($[\text{J mol}^{-1}]$ or $[\text{kJ mol}^{-1}]$), R is the universal gas constant [$8.314 \text{ J mol}^{-1} \text{ K}^{-1}$], T is the absolute temperature [K], makes the implicit assumption that the temperature dependence of the rate constant, $k(T) = A \cdot \exp(-E_a/RT)$ [Eq. (1)], can be separated from reaction model function, $f(\alpha)$. Several examples of reaction model functions are given in literature

(Bamford and Tipper 1980). Extent of conversion or the conversion fraction (α), $0 \leq \alpha \leq 1$, is a global parameter typically evaluated from mass loss or reaction heat (α determined from TGA runs as a fractional mass loss: $\alpha = (m_o - m_t)/(m_o - m_f)$, where m_o is the initial mass of the sample measured in TGA experiments, m_t is mass of the sample in time t , and m_f is the final mass of the sample, measured at the end of considered TGA run).

Isoconversional methods, also referred as “model-free” methods, were developed to extract the kinetic information without the need of the reaction model by comparing the measurements made a common extent of conversion under two or more sets of different conditions.

Under the isothermal conditions, a standard integral isoconversional method (Vyazovkin and Wight 1997), can be readily derived from logarithmic form of the integral rate-law equation [Eq. (1)] as $g(\alpha) = A \cdot \exp(-E_a/RT) \cdot t$ (where $g(\alpha)$ is integral form of reaction model function), with $k(T)$ substituted by the Arrhenius equation:

$$-\ln t_{\alpha,i} = \ln \left[\frac{A}{g(\alpha)} \right] - \frac{E_{a,\alpha}}{RT_i}, \quad (2)$$

where i is the ordinal number of two or more isothermal experiments. At each α , $E_{a,\alpha}$ is evaluated from the slope of $-\ln t_{\alpha,i}$ versus $1/T_i$ plot, while in this case the A (the pre-exponential) cannot be directly computed without acquiring the exact form of $g(\alpha)$.

The Friedman’s differential isoconversional method (Friedman 1963) does not involve solving the temperature integral (Flynn 1997). It is applicable for isothermal as well as non-isothermal conditions. By taking the natural logarithm of Eq. (1), we have the isothermal form of the Friedman equation, as:

$$\ln \left(\frac{d\alpha}{dt} \right)_{\alpha,i} = \ln[A_\alpha \cdot f(\alpha)] - \frac{E_{a,\alpha}}{RT_i}. \quad (3)$$

A dependence of $E_{a,\alpha}$ on α , can be obtained by evaluating the E_a over a full range of α , from 0 to 1. Although, the Friedman’s isoconversional method does not make any mathematical approximation, it is usually very sensitive to the experimental perturbations related to the measurements of the reaction rates ($d\alpha/dt$). Additional uncertainties may be introduced, especially when the numerical smoothing of experimental data is applied.

Solid state reactions often undergo self-heating processes that lead to distorted linear heating program. In such cases, the heating rate can be hardly maintained as a constant during a prescribed linear heating experiment. To address this issue, Vyazovkin’s (1997a) extended the non-linear isoconversional method to deal with arbitrary heating programs, including isothermal conditions. So, Eq. (1) can be expressed in its integral form:

$$g(\alpha) = A_\alpha \int_0^{t_\alpha} \exp \left[-\frac{E_a}{RT(t)} \right] dt = A_\alpha \cdot J[E_{a,\alpha}, T(t_\alpha)]. \quad (4)$$

By assuming the reaction model is independent of temperature and heating rate, we have:

$$g(\alpha) = A_\alpha \cdot J[E_a, T_i(t_\alpha)] = \text{const.}, \quad i = 1, \dots, n \quad (5)$$

The E_a values are then determined at any given α by finding an $E_{a,\alpha}$ such that it minimizes the function $\Phi(E_a)$:

$$\Phi(E_a) = \sum_{i=1}^n \sum_{j \neq i}^n \frac{J[E_{a,\alpha}, T_i(t_\alpha)]}{J[E_{a,\alpha}, T_j(t_\alpha)]} = \min. \quad (6)$$

The temperature integral, $J[E_{a,\alpha}, T(t_\alpha)]$, is evaluated by the numerical integration with all available discrete experimental measurements at $T = \text{const.}$, and $\alpha = \text{const.}$, at the corresponding time values. As one would notice, the $E_{a,\alpha}$ evaluated by all these isoconversional methods mentioned above, regardless of their accuracy, is an average over the full region from 0 to α . Identifying the variations in the apparent activation energy is a characteristic advantage of isoconversional methods. However, the magnitude of such variations may be gradually flattened out as a reaction approaches its end. In this respect, Vyazovkin (1997b, 2001) further proposed a modification to the non-linear isoconversional method (modified non-linear isoconversional method) to overcome this issue. In Eq. (4), the regular integral from 0 to t_α is replaced with an integral over a small time interval:

$$J[E_{a,\alpha}, T(t_\alpha)] = \int_{t_\alpha - \Delta\alpha}^{t_\alpha} \exp \left[-\frac{E_a}{RT(t)} \right] \cdot dt. \quad (7)$$

Integral in Eq. (7) is evaluated by numerical integration for various heating programs or the

isothermal temperatures and then plugged into Eq. (6). Minimization procedure is performed to find the optimal $E_{a,\alpha}$ for a given α . In the current method, $E_{a,\alpha}$ is assumed to be constant only within a small segment of $\Delta\alpha$. Dependence of the apparent activation energy on the entire conversion fraction (α) can be derived by repeating the procedure for each α as it steps by $\Delta\alpha$ from 0 to 1.

By varying the $E_{a,\alpha}$, then we are able to find an optimal $E_{a,\alpha,\min}$ that minimizes the variance and gives: $\chi_{\min}^2 = \chi^2(E_{a,\alpha,\min})$. A statistic can be constructed as:

$$\Psi(E_{a,\alpha}) = \frac{\chi^2(E_{a,\alpha})}{\chi_{\min}^2}, \quad (8)$$

and it should follow F-distribution. Hence, we can evaluate the lower and upper confidence bounds for $E_{a,\alpha}$ based on F-test, within 95 % of confidence limits. Any value of $E_{a,\alpha}$ that satisfies $\Psi(E_{a,\alpha}) < F_{1-p,n-1,n-1}$ is considered statistically equivalent to $E_{a,\alpha,\min}$ with $(1-p) \cdot 100$ % confidence probability (where n is the total number of experiments, $(n-1)$ is the total number of terms in a single summation, p represents the probability of success, while $(1-p)$ is the complement of the event).

Theory of Bayesian inference

Suppose the data $X = (x_1, \dots, x_n) \equiv (\varepsilon_{a,1}, \dots, \varepsilon_{a,n})$ (where x_1, \dots, x_n actually correspond to $\varepsilon_{a,1}, \dots, \varepsilon_{a,n}$) (where the scalar x corresponds to energy counterpart ε_a) represent the realizations of a random variable with a density from the parametric family $F = \{f(\varepsilon_a; \theta): \theta \in \Omega\}$ (where θ is unknown parameter, which belongs to the parameter vector $\omega \in \Omega$ within parameter space, which depends on the number of unknown parameters θ ; the functional form of f is fully specified up to a parameter θ).

Based on Bayes theorem (Aven and Kvaløy 2002), the un-observable parameters in a statistical model can be treated as random. When no data are available, a prior distribution is used to quantify our knowledge about the parameter. When data are available, we can update our prior information using conditional distribution of parameters, given by the data. Transition from the prior to posterior is possible through Bayes theorem (Lester et al. 2003; Langston et al. 2001).

If we assume that before a given experiment, our prior distribution describing parameter θ is $\pi(\theta)$. The

data are accompanied by superior model (the likelihood), which depends on the parameter and is usually celebrated with $f(\varepsilon_a|\theta)$. Bayes theorem updates prior $\pi(\theta)$ to posterior by accounting for the data ε_a in the form:

$$\pi(\theta|\varepsilon_a) = \frac{f(\varepsilon_a|\theta)\pi(\theta)}{m(\varepsilon_a)}, \quad (9)$$

where $m(\varepsilon_a)$ is a normalized constant, $m(\varepsilon_a) = \int_{\omega} f(\varepsilon_a|\theta) \cdot \pi(\theta) d\theta$.

Once the data ε_a available to us, θ is only unknown quantity and posterior distribution $\pi(\theta|\varepsilon_a)$ completely describes the uncertainty. There are two key advantages of Bayesian approach: [A] once the uncertainty is expressed via the probability distribution and statistical inference can be automated, it follows a conceptually simple recipe, and [B] available prior information is coherently incorporated into the statistical model.

The corresponding model for observation $X (\equiv E_a)$ conditioned by unknown parameter θ is density function $f(\theta|\varepsilon_a)$. As a function of θ , $f(\theta|\varepsilon_a) = L(\theta)$ is usually called likelihood. According to likelihood principle (Royall 1997; Mayo 2010), all experimental information about the data must be contained in likelihood function. The parameter θ with the values in the parameter space Ω are taken as random variables. The random variable θ has a distribution $\pi(\theta)$ called the prior distribution. Prior describes uncertainty about the parameter before the data are observed. If prior for θ is specified up to a parameter τ , $\pi(\theta|\tau)$, for that matter, τ is called as hyperparameter.

The aim is to start with this prior information and update it using the data to make the best possible estimator of θ . This can be achieved using likelihood function to get $\pi(\theta|\varepsilon_a)$, what is called posterior distribution, for a given $E_a = \varepsilon_a$. The name ‘‘posterior distribution’’ hints role $\pi(\theta|\varepsilon_a)$. As a prior distribution reflects certificate about θ before experiment, thus $\pi(\theta|\varepsilon_a)$ reflects certificate about θ after obtaining an $(\varepsilon_{a,1}, \dots, \varepsilon_{a,n})$ pattern. In other words, the posterior distribution combines a priori beliefs of θ and information about θ contained in the realized data ‘sample’, in order to obtain the final ‘‘image’’ of θ . Thus, implicitly assumes that there is a principle of credibility or, in other words, it is assumed that all sampling information about θ contained in $f(\varepsilon_a|\theta)$ (for

a given ε_a). In search of $\pi(\theta|\varepsilon_a)$, we benefit the Bayes rule that would delimit the joint distribution for E_a and θ [$h(\varepsilon_a, \theta) = f(\varepsilon_a|\theta)\pi(\theta)$] for marginal distribution $m(\varepsilon_a)$, whereby this can be obtained by integrating out parameter θ from joint distribution $h(\varepsilon_a, \theta)$ such as:

$$m(\varepsilon_a) = \int_{\omega} h(\varepsilon_a, \theta)d\theta = \int_{\omega} f(\varepsilon_a|\theta)\pi(\theta)d\theta. \tag{10}$$

Marginal distribution is often called the prior predictive distribution. Finally, we can get the expression for posterior distribution, $\pi(\theta|\varepsilon_a)$:

$$\pi(\theta|\varepsilon_a) = \frac{h(\varepsilon_a, \theta)}{m(\varepsilon_a)} = \frac{f(\varepsilon_a|\theta)\pi(\theta)}{m(\varepsilon_a)} = \frac{f(\varepsilon_a|\theta)\pi(\theta)}{\int_{\omega} f(\varepsilon_a|\theta)\pi(\theta)d\theta}. \tag{11}$$

Table 1 summarizes the ingredients of Bayesian inference (notation) used in this paper.

In addition, if $\pi(\theta)$ is uniform—that is, the same for all θ , then expression on the final right-hand side of Eq. (11) simplifies to

$$\frac{f(\varepsilon_a|\theta)}{\int_{\omega} f(\varepsilon_a|\theta)d\theta}. \tag{12}$$

The above ratio is called the standardized or the normalized likelihood function (Karabatsos and Walker 2006; Myung et al. 2006), provided that $\int_{\omega} f(\varepsilon_a|\theta)d\theta$ is finite.

The main starting point for setting the calculation procedure in order to obtain all Bayesian ingredients for investigated process is based on the following:

Table 1 The defined ingredients of Bayesian inference (notation) used in the current research

Bayesian inference		
Name	Notation	Equal to
Likelihood	$f(\varepsilon_a \theta)^a$	
Prior distribution	$\pi(\theta)$	
Joint distribution	$h(\varepsilon_a, \theta)$	$f(\varepsilon_a \theta) \cdot \pi(\theta)$
Marginal distribution	$m(\varepsilon_a)$	$\int_{\omega} f(\varepsilon_a \theta) \cdot \pi(\theta)d\theta$
Posterior distribution	$\pi(\theta \varepsilon_a)$	$f(\varepsilon_a \theta) \cdot \pi(\theta)/m(\varepsilon_a)$

^a Likelihood is based on the likelihood function. Since, it is not a probability density, then it may decide that it is the best estimator of the parameter is the value that has the highest value of the likelihood function

Since the distribution type of the pyrolysis process is unknown, we have to make a initial assumption about the possible shape of the function $f(\theta|\varepsilon_a)$, with unknown or maybe “virtual” parameters θ . This “estimation” can be obtained from isoconversional analysis [primarily from the modified non-linear Vyazovkin’s method, keeping in mind that this approach uses a larger number of conversion fraction (α) values and therefore we have a greater number of calculated E_a values, where the sample size is equal to 100 (hundred ε_a counterparts); also, this approach severely reduces the systematic error observed in other integral/differential isoconversional methods (see above)]. After receiving the isoconversional dependency $E_{a,\alpha} = E_{a,\alpha}(\alpha)$, then differentiating the dependence $\alpha = \alpha(E_{a,\alpha})$ in respect to E_a ($d\alpha(E_{a,\alpha})/dE_{a,\alpha}$) we can obtain the initial form of $f(\theta|\varepsilon_a)$, with generally unknown θ . Based on the shape of the curve which was evaluated, we then assume the type of distribution. The strategy is to select those which can provide a more conservative estimates, accompanied with maximum likelihood estimates (MLE) (states the model) (Aldrich 1997), and then the calculations which occur in the completion of the distributions within the Bayesian inference (Table 1), and which will be presented in the next section of this paper. The advantage of this approach is that the Bayesian inference estimates a full probability model, which can directly assist in the interpretation of the exact mechanistic scheme of the pyrolytic process. The Bayesian inference framework allows us to improving the important parameters estimation (Tang and Zhuang 2009), which reflects the kinetic behavior of the cellulose molecules during isothermal pyrolysis, wherein determining the course of a comprehensive mechanism of the process, i.e. the prediction of the same.

In this paper, it is preferably assumed that probability distributions may be described through their probability density functions, and no distinction is made between a random quantity and the particular values that it may take. Moreover, the standard mathematical convention of referring to functions, pronounce f of $\varepsilon_a \in E_a$ will be used in this work. Density functions of specific distributions are denoted by appropriate names. Thus, if ε_a is a random quantity with a normal distribution of mean μ and standard deviation σ , its probability density function will be denoted by $\mathcal{N}(\varepsilon_a|\mu, \sigma)$.

Results and discussion

Thermo-kinetic characteristics of the pyrolysis rate curves

Figure 1 shows the experimentally obtained rate-time curves for the powdered cellulose pyrolysis, at various operating temperatures (300, 320, 330 and 340 °C).

From Fig. 1 we can see that all recorded rate-time curves at all observed operating temperatures show decreasing behavior with time, according to nearly exponentially decay laws. For all operating temperatures, the maximum rate (v_{max}) reaches its value $v = v_{max}$ at $t = 0$. It should be noted that various types of kinetic models are conventionally placed into two main groups: $\alpha - t$ relationships that give either (i) sigmoid or (ii) deceleratory curves (Khawam and Flanagan 2006). These expressions, $g(\alpha) = k \cdot t$, may be differentiated to give the expressions $f(\alpha) = v/k$ (where $v \equiv d\alpha/dt$; k is the rate constant), and by suitable substitution, these may be expressed as functions of time, $v = h(t)$. Within the deceleratory group of kinetic models (including the first-order (F1) and “ n th” order (reaction order different from the unity) (Fn) reaction models, geometrical contraction [R2 (contracting area) and R3 (contracting volume)] reaction models, and diffusion (D1, D2, D3 and D4) reaction models) (Khawam and Flanagan 2006) have $v = v_{max}$ at $t = 0$. This characteristic feature exhibits all the rate-time curves in Fig. 1. A secondary feature, analogous to *half-life* ($t_{1/2}$), in the conventional kinetic

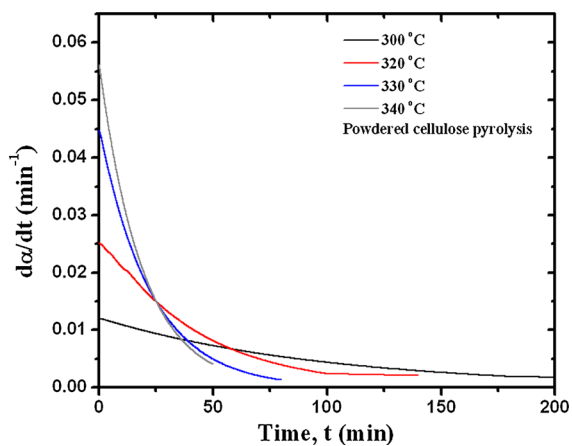


Fig. 1 The experimentally obtained rate-time curves for the powdered cellulose pyrolysis, at various operating temperatures (300, 320, 330 and 340 °C)

analysis, is the time value, $t_{m/2}$, taken for the rate to drop to half its maximum value (i.e., $v_{max}/2$). The rate-time features, such as v_{max} , $v_{max}/2$ and $t_{m/2}$, may be determined from experimental pyrolysis data, without knowledge of the particular kinetic model that applies to the data, other than the visually obvious classification into one or the other of the two main groups. Based on the shapes and specific properties of the rate-time curves shown in Fig. 1, we can unambiguously conclude that the mechanism of powdered cellulose pyrolysis process follows the deceleratory kinetic behavior.

The essential difference between the rate-time curves shown in Fig. 1 is reflected in their slopes, which directly affect values of pyrolysis rates in certain parts of the rate curves at various operating temperatures, and also on the values of $t_{m/2}$. Table 2 lists the values of the rate-time features (v_{max} , $v_{max}/2$ and $t_{m/2}$) at the different operating temperatures for the pyrolysis of powdered cellulose samples.

It can be seen from Table 2 that the values of v_{max} and $v_{max}/2$ increase with an increasing of operating temperature, where the absolute maximum rate of pyrolysis (v_{max}) is achieved at the highest value of the operating temperature (at 340 °C). On the other hand, the value of $t_{m/2}$ decreases with an increasing of the operating temperature, in respect to the exponential decay process, which is typical for the rates of certain types of chemical reactions depend on the concentration of one reactant. Reactions whose rate depends only on the concentration of one reactant (known as first-order reactions) consequently follow exponential decay. Deviation from the mechanism of the process being modeled by reaction of the first order going to a non-integer reaction orders may indicates a

Table 2 The rate-time curve features (v_{max} , $v_{max}/2$ and $t_{m/2}$) at different operating temperatures (300, 320, 330 and 340 °C), for the isothermal pyrolysis of the powdered cellulose samples

Powdered cellulose			
T (°C)	v_{max} (min ⁻¹)	$v_{max}/2$ (min ⁻¹)	$t_{m/2}$ (min)
300	0.01198	0.00544	78.20
320	0.02514	0.01098	37.69
330	0.04486	0.01610	23.52
340	0.05623	0.02162	18.23
Average	0.03455	0.01353	39.41

more complex reaction mechanism, that may involves a concentrations of more than one reaction species.

The results presented in Table 2 have been validated through the application of the first-order kinetic model (F1), where $t_{m/2} = (\ln 2)/k \equiv t_{1/2}$ whereby we get $\alpha = 1 - \exp(-k \cdot t)$ [k is the rate constant in (min^{-1})] (the above expression represents the relation for estimation of conversion fraction (α) values, which belongs to the first-order reaction mechanism).

Figure 2 shows the comparison between the experimentally obtained and calculated [taking into account the relation $\alpha = 1 - \exp(-k \cdot t)$] conversion ($\alpha - t$) curves for the pyrolysis process of powdered cellulose at the different operating temperatures, where it is assumed validity of the first-order (F1) reaction mechanism. At the same figure, the corresponding rate constant (k) values calculated for F1 kinetic model are also presented.

From Fig. 2 we can see that there is quite a large discrepancy between the experimental and calculated conversion curves, related to the first-order kinetics. The presented results clearly indicate that the first-order kinetics does not hold for the pyrolysis process attached to powdered cellulose. Based on these results, we can conclude that the kinetics of cellulose pyrolysis is much more complicated than can be described by the first-order (F1) kinetic model.

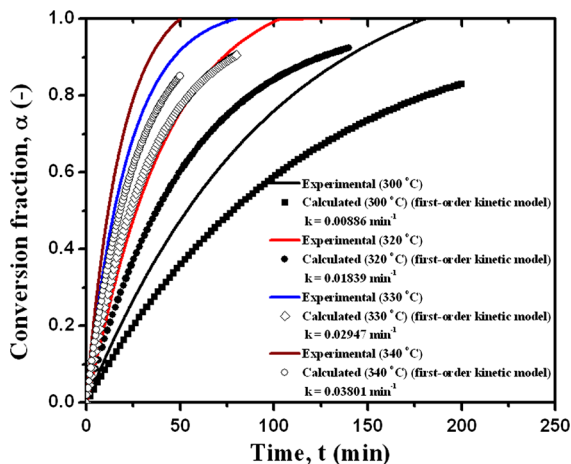


Fig. 2 The comparison between the experimentally obtained and calculated [taking into account the relation $\alpha = 1 - \exp(-k \cdot t)$] conversion ($\alpha - t$) curves for the pyrolysis process of the powdered cellulose at the different operating temperatures (300, 320, 330 and 340 °C), where it is assumed validity of the first-order (F1) reaction mechanism. At the same figure, the corresponding rate constant (k) values, calculated for the first-order kinetic model are also presented

It should be noted that the reciprocal of the $t_{m/2}$ value (i.e., $t_{m/2}^{-1}$) is usually used to describe the overall rate of the isothermal pyrolysis process. From the linear dependence such as $\ln(1/t_{m/2}) = \text{const.} - E_{a,\text{cellulose}}/RT_i$, we can calculate the overall apparent activation energy value for pyrolysis process of powdered cellulose samples (designated by $E_{a,\text{cellulose}}$). The corresponding linear plot of the above-stated linear relationship, with appropriate 95 % confidence limits for powdered cellulose pyrolysis is illustrated in Fig. 3.

It can be seen from Fig. 3 that fairly good linear correlation exists, where all data are contained within the predetermined 95 % confidence limits. The resulting error in the $E_{a,\text{cellulose}}$ value (Fig. 3) is in the limits of the experimental errors. The obtained value of the overall apparent activation energy for the investigated pyrolysis process amounts $E_{a,\text{cellulose}} = 108.9 \pm 0.7 \text{ kJ mol}^{-1}$ (Fig. 3).

Table 3 summarizes the results of apparent activation energies and reaction orders for cellulose pyrolysis process, obtained under non-isothermal and isothermal experimental conditions. Results were sublimed from a variety of available literatures and these results are compared with the results reported in this work.

It can be found that the apparent activation energies for cellulose pyrolysis are typically ranged from $E_a = 93.0 \text{ kJ mol}^{-1}$ up to $E_a = 278.5 \text{ kJ mol}^{-1}$,

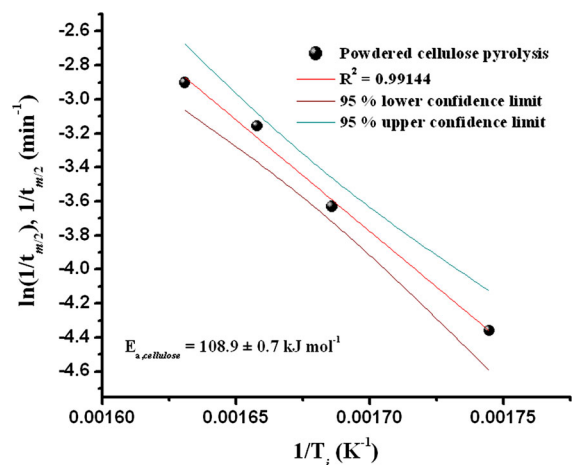


Fig. 3 The linear dependence of $\ln(1/t_{m/2})$ versus $1/T_i$ for the isothermal pyrolysis process of the powdered cellulose. The corresponding overall apparent activation energy value ($E_{a,\text{cellulose}}$) is also indicated

which greatly depends on the specific experimental conditions, the range of used (dynamic/static) temperatures, the gas partial pressures etc. Generally speaking, the obtained result in the present work is in reasonable ranges when compared to other studies (Table 3). However, it should be emphasized that the chemical kinetics in other studies was developed mainly on the non-isothermal (dynamic) thermal decomposition, whereas the currently obtained result pertains to isothermal kinetics. However, if we only look at the results related to the isothermal kinetics, the value of E_a obtained here for the considered cellulose samples is completely logical and totally acceptable.

Isoconversional analysis

Figure 4 shows the isoconversional dependence of the apparent (effective) activation energy values ($E_{a,\alpha}$) on the conversion fraction (α) for the isothermal pyrolysis of powdered cellulose. The observed isoconversional dependencies are estimated from the standard (integral) (symbol *square*) and Friedman's (differential) (symbol *circle*) isoconversional methods [Eqs. (2, 3)].

In addition, Fig. 5 shows the isoconversional dependence $E_a = E_a(\alpha)$ evaluated by the advanced Vyazovkin's modified non-linear isoconversional approach, for the pyrolysis process of powdered cellulose. The calculation procedure was conducted with steps by $\Delta\alpha = 0.01$ from 0.05 to 0.95 of the total conversion values. In the current figure, the corresponding 95 % confidence limits, with lower and upper bounds are clearly marked.

It can be seen from Fig. 4 that the course of the apparent activation energy values depends on the conversion fraction. Curves that show the apparent activation energies, obtained by two different isoconversional methods have a similar course (Fig. 4). In the initial stage of pyrolysis process (up to $\alpha = 0.10$), an increase in E_a values in both curves occurs. After their short consolidation, there is a slow decrease in E_a values (from $\alpha = 0.10$ to $\alpha = 0.30$) and then short "stabilization" at $\alpha = 0.35$ (Fig. 4). Starting from $\alpha = 0.45$, a significant decrease in E_a values can be observed [valid for both considered methods (Fig. 4)].

For a conversion fraction values in the range of $\alpha = 0.05$ – 0.10 , an increasing dependence of E_a on α

Table 3 Summary of the reaction orders (plus additional kinetic models) and apparent activation energies for cellulose pyrolysis process under isothermal and non-isothermal experimental conditions

Material	T (°C)	Reaction order (n) ^c	E_a (kJ mol ⁻¹)	References
Cellulose	200–270 ^a	0.80	93.0	Muller-Hagedorn et al. (2003)
	253–394 ^a	1.00	278.5	Mui et al. (2010)
	230–380 ^a	1.00	185.0	Sonobe and Worasuwanarak (2008)
	300–340 ^a	1.00	227.0	Yang et al. (2004)
	200–300 ^b	1.00	124.4	Chen and Kuo (2011)
	280–400 ^a	1.00	124.6	Poletto et al. (2012)
	50–650 ^a	1.00	203.0	Shaik et al. (2013)
	30–700 ^a	<i>Non-reaction order</i> /autocatalytic Prout-Tompkins model	200.0	Capart et al. (2004)
	280–320 ^b	<i>Non-reaction order</i> /autocatalytic Prout-Tompkins model	203.0	Capart et al. (2004)
	260–275 ^b	<i>Non-reaction order</i> /Chain scission model (L2)	191.0	Sánchez-Jiménez et al. (2013)
	360–370 ^b	<i>Non-reaction order</i> /Nucleation and growth model (Avrami-Erofeev) (A3.69)	193.0	Kim and Eom (2006)
	300–340 ^b	$n \neq 1$	108.9	Present study

^a Non-isothermal kinetics

^b Isothermal kinetics

^c ("n") models that include reaction orders, but same table also incorporates and other types of identified kinetic models

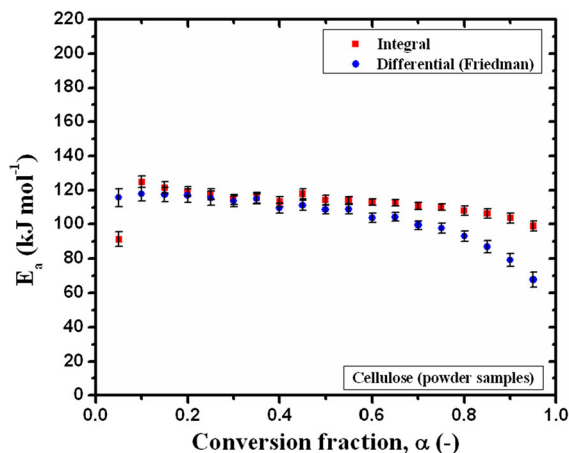


Fig. 4 The isoconversional dependence of the apparent (effective) activation energy values ($E_{a,\alpha}$) on the conversion fraction (α) for the isothermal pyrolysis of the powdered cellulose. The observed isoconversional dependencies are estimated from the standard (integral) (symbol *square*) and Friedman's (differential) (symbol *circle*) isoconversional methods

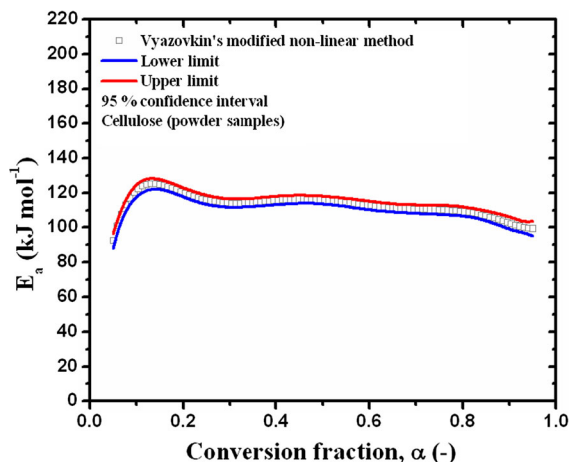


Fig. 5 The isoconversional dependence $E_a = E_a(\alpha)$ evaluated by the advanced Vyazovkin's modified non-linear isoconversional approach, for the isothermal pyrolysis process of the powdered cellulose. The calculation procedure was conducted with steps by $\Delta\alpha = 0.01$ from 0.05 to 0.95 of the total conversion values. In the current figure, the corresponding 95 % confidence limits, with lower and upper bounds are clearly marked

obviously can be observed. This behavior is characteristic of competing reactions (Vyazovkin 1996). This segment corresponds to the start of cellulose pyrolysis. It is affected by competition among the decomposition of individual macromolecules and the inter-molecular associates. In addition, it should be

noted that the later decrease in E_a with α (with lower conversions) can be attributed to the ongoing depolymerization of cellulose molecules.

It should be noted that for the values of conversion fraction above $\alpha \geq 0.70$, the slightly lower values of Adj. R-Square (R^2) attached to isoconversional plots were obtained (not shown here). For these values of R^2 and given α 's, the decline in E_a values with α were identified, which is particularly evident in the case of differential (Friedman's) method (Fig. 4). Regarding the mentioned facts related to the lower values of the R^2 , these parts of the curves ($\alpha \geq 0.70$) do not provide sufficient evidence, and it would be confusing to consider them as accurate. It should be noted that in the case of both applied methods, the minimal variations of E_a with α were observed in the range of conversions from $\alpha = 0.20$ to $\alpha = 0.65$, where in a given α range, the average value of the difference in E_a values calculated by considered methods is only 4.5 kJ mol^{-1} , which is quite acceptable for any errors that may occur when applying these methods. In the considered range of conversions, the apparent activation energy value may be taken as constant. The following values of E_a were obtained: $\langle E_a \rangle^{Int} = 115.2 \pm 2.7 \text{ kJ mol}^{-1}$ and $\langle E_a \rangle^{Friedman} = 110.7 \pm 3.0 \text{ kJ mol}^{-1}$ (where "Int" and "Friedman" are attached to the *integral* and *differential* (Friedman's) isoconversional methods). The value of E_a calculated by the Friedman's method ($110.7 \text{ kJ mol}^{-1}$) is in quite good agreement with the value of $E_{a,cellulose}$ ($108.9 \text{ kJ mol}^{-1}$; see above). We also need to say that the values of E_a , which are calculated using the advanced Vyazovkin's modified non-linear isoconversional method (Fig. 5) are in excellent agreement with the values of E_a calculated by the previous two isoconversional methods, where $E_a = E_a(\alpha)$ dependence has almost identical trend as the ones in Fig. 4. There are often higher values of the apparent activation energy of cellulose pyrolysis in the literature (Table 3). It may be a consequence of various conditions during the measurement, mainly the different weights of the samples and different nature and flow velocities of the atmosphere, in which the test takes place.

The apparent activation energies obtained by isoconversional methods at lower conversions ($\alpha < 0.20$) and higher conversions ($\alpha > 0.70$) were found to be noticeably different from the apparent activation energies (almost constant) obtained in the range $\alpha = 0.20$ – 0.65 . This indicates the different

mechanisms of cellulose decomposition at lower conversion (dehydration and depolymerization), moderate conversion (decomposition of cellulose and competition between formation of volatile compounds and char) and higher conversion (cross-linking and aromatic cyclization of char residue). In the conversion ranges, where nearly constant values of E_a were identified (Figs. 4, 5), we can expect that a similar mechanism is operating in these ranges ($\alpha = 0.20$ – 0.65). Many researchers (Liau and Hsieh 2005; Khachani et al. 2014) have reported an average value of E_a , but we must bear in mind that due to the occurrence of many different elementary steps and complex mechanisms of thermal decomposition of cellulose, it is not appropriate to give an average value of E_a . The variation in E_a is justified because of the different elementary steps and complex mechanisms of thermal decomposition process. In the present study, the above established average values of E_a ($\langle E_a \rangle^{Int}$ and $\langle E_a \rangle^{Friedman}$) should be understood as the “lumped” kinetic parameters. However, it is necessary to prove whether derived average values of E_a in the observed range of conversion fraction values are really “lumped” kinetic parameters, or they may with reasonable grounds taken as real (‘true’) kinetic parameters that can be joined correctly to the evaluated reaction mechanism function, which can realistically describe the tested pyrolysis process.

The exact analytical form of the reaction mechanism function can not be determined solely on the basis of isoconversional analysis, but this requires an additional considerations.

Searching for the real form of the reaction mechanism function

Since we have proved that the pyrolysis process of powdered cellulose can not be described with first order kinetics, then we are obliged to carry out the checking procedure, whether the process is subject to the kinetics which obeys a mechanism that involves reactions that deviate from the first-order. If the order of reaction is not unity, the integration of basic rate law equation, $d\alpha/dt = k \cdot (1 - \alpha)^{n^*}$ (where n^* represents the apparent reaction order) becomes

$$(1 - \alpha)^{1-n^*} - 1 = (n^* - 1)k \cdot t. \quad (13)$$

The plot of $[(1 - \alpha)^{1-n^*} - 1]$ versus t gives a straight line with a slope equal to $(n^* - 1) \cdot k$. Accordingly, the rate constants at various operating temperatures (T_i) can be calculated. From the logarithmic form of the Arrhenius equation, $\ln(k) = \ln A - E_a/RT_i$, the kinetic parameters, $\ln A$ or A (the pre-exponential factor) and the apparent activation energy E_a can be calculated, from the plot of $\ln(k)$ versus T_i^{-1} , which gives a straight line (the slope of the line is equal to $-E_a/R$, and the intercept is equal to $\ln A$). These kinetic parameters may then be compared with the results of the analysis carried out by means of isoconversional approach, for the purpose of comparing the values of E_a .

Table 4 lists the results obtained from the application of $[(1 - \alpha)^{1-n^*} - 1]$ versus t plots analyses, for a various values of the apparent reaction orders (n^*), ranged from 0.25 to 4.00, in the case of the tested pyrolysis process. Same table also shows the results of statistical analysis, which includes the Adj. R-Square (R^2) and Fisher (F)-test values. All results are presented for all considered operating temperatures.

We can see from Table 4 that is undoubtedly the best model was the one that has a apparent reaction order which is less than unity ($n^* < 1$), and which is equal exactly to $n^* = 0.75$ ($n^* = 6/8$). This result clearly confirms that the mechanism of powdered cellulose pyrolysis can be best described with reaction order mechanism different from the unity ($n^* \neq 1$, i.e., for $n^* < 1$). In addition, Table 5 lists the values of calculated rate constant (k) values, which were estimated from the results presented in the Table 4, for all considered operating temperatures (300, 320, 330 and 340 °C).

In the current table, the best selected rate constant (k) value at every considered operating temperature, for $n^* = 0.75$, is clearly marked, with *bold* tags. Figure 6 shows the dependence of $\ln(k)$ versus $1/T_i$ for the values of k which correspond to the selected apparent reaction order ($n^* = 0.75$) (see Table 5). In Fig. 6, only the roughly dependence, without establishing a linear-regression analysis to a given experimental points was shown.

From Fig. 6 we can see the effect of n^* at the rate constant (k) with a change in operating temperature values. Namely, in our considered case, it is important to note that the value of n^* less than unity tends to introduce a “new”, the ‘reverse’ curvature in the

Table 4 The results obtained from the application of $[(1 - \alpha)^{1-n^*} - 1]$ versus t plots analyses, for a various values of the apparent reaction orders (n^*), ranged from 0.25 to 4.00, in the case of isothermal powdered cellulose pyrolysis (calculation procedure was applied for conversion range of $\alpha = 0.20-0.65$)

n^*	300		320		330		340		300		320		330		340	
	$(n^* - 1) \cdot k^a$	$(n^* - 1) \cdot k^a$	$(n^* - 1) \cdot k^a$	$(n^* - 1) \cdot k^a$	$(n^* - 1) \cdot k^a$	$(n^* - 1) \cdot k^a$	$(n^* - 1) \cdot k^a$	$(n^* - 1) \cdot k^a$	F^c	R^{2b}	F^c	R^{2b}	F^c	R^{2b}	F^c	R^{2b}
0.25	-0.00656	-0.01354	-0.02203	-0.02841	0.99716	10166.8	0.99548	4404.1	0.99367	3456.9	0.99511	5494.3				
0.50	-0.00508	-0.01050	-0.01712	-0.02212	0.99932	42686.5	0.99844	12817.3	0.99739	8393.5	0.99824	15293.9				
0.75 ^d	-0.00296	-0.00612	-0.01001	-0.01294	1.00000	6.6×10^6	0.99990	1.5×10^5	0.99950	43285.4	0.99984	1.4×10^5				
1.15	0.00228	0.00471	0.00774	0.01004	0.99792	13930.9	0.99889	17924.8	0.99941	40218.7	0.99900	27417.5				
1.25	0.00404	0.00837	0.01376	0.01785	0.99680	9026.9	0.99801	10038.5	0.99879	18091.9	0.99818	14816.7				
1.50	0.00947	0.01963	0.03240	0.04208	0.99293	4076.5	0.99474	9781.7	0.99597	5444.5	0.99499	5362.3				
1.75	0.01669	0.03463	0.05733	0.07455	0.98760	2310.9	0.98994	1968.6	0.99156	2587.0	0.99025	2743.2				
2.00	0.02620	0.05443	0.09039	0.11769	0.98085	1486.7	0.98366	1205.2	0.98561	1507.7	0.98402	1663.3				
2.25	0.03865	0.08037	0.13391	0.17456	0.97274	1036.0	0.97598	813.8	0.97818	987.4	0.97636	1116.2				
2.50	0.05485	0.11418	0.19091	0.24912	0.96337	763.7	0.96698	586.8	0.96938	697.4	0.96737	801.5				
2.75	0.07583	0.15805	0.26520	0.34642	0.95282	586.7	0.95676	443.6	0.95929	519.5	0.95714	604.0				
3.00	0.10293	0.21477	0.36171	0.47294	0.94120	465.2	0.94543	347.5	0.94805	402.5	0.94579	472.1				
3.25	0.13781	0.28791	0.48671	0.63697	0.92862	378.3	0.93309	279.9	0.93577	321.5	0.93343	379.6				
3.50	0.18262	0.38199	0.64823	0.84912	0.91519	313.9	0.91987	230.6	0.92257	263.1	0.92019	312.3				
3.75	0.24006	0.50278	0.85657	1.12298	0.90103	265.0	0.90587	193.5	0.90859	219.7	0.90618	261.8				
4.00	0.31359	0.65762	1.12488	1.47595	0.88625	226.9	0.89126	164.9	0.89394	186.4	0.89153	222.9				

^a Slope The plot of $[(1 - \alpha)^{1-n^*} - 1]$ versus t

^b Adj. R-Square

^c Fisher (F) statistical test

^d Statistical best kinetic model which is associated with the corresponding best selected apparent reaction order; with *bold* numbers were labeled the best statistical parameters

Table 5 The rate constant (k) values at various operating temperatures (300, 320, 330 and 340 °C), calculated for every observed apparent reaction order (n^*) value, for isothermal pyrolysis process of the powdered cellulose

Temperature, T (°C)				
n^*	300 k (min ⁻¹)	320 k (min ⁻¹)	330 k (min ⁻¹)	340 k (min ⁻¹)
0.25	0.00875	0.01805	0.02937	0.03788
0.50	0.01016	0.02100	0.03424	0.04424
0.75 ^a	0.01184	0.02448	0.04004	0.05176
1.15	0.01520	0.03140	0.05160	0.06693
1.25	0.01616	0.03348	0.05504	0.07140
1.50	0.01894	0.03926	0.06480	0.08416
1.75	0.02225	0.04617	0.07644	0.09940
2.00	0.02620	0.05443	0.09039	0.11769
2.25	0.03092	0.06430	0.10713	0.13965
2.50	0.03657	0.07612	0.12727	0.16608
2.75	0.04333	0.09031	0.15154	0.19795
3.00	0.05147	0.10739	0.18085	0.23647
3.25	0.06125	0.12796	0.21631	0.28310
3.50	0.07305	0.15280	0.25929	0.33965
3.75	0.08729	0.18283	0.31148	0.40836
4.00	0.10453	0.21921	0.37496	0.49198

^a The best rate constant values for investigated pyrolysis process, at different T_i 's, for appropriate value of n^*

current “plot” at the high operating temperatures ($T_i \geq 330$ °C [603.15 K]; Fig. 6). The actual value of n^* which is less than unity [but not significantly below of $n^* = 1.00$ (where n^* will not fall below 0.50)] slightly increases the overall downward curvature, as can be seen in Fig. 6. Now we can ask whether the effect of n^* in respect to its magnitude can affects the quality of the linear regression and in the error sizes of the calculated kinetic parameters, from the logarithmic form of the Arrhenius equation.

Figure 7 shows the plot of $\ln(k)$ versus $1/T_i$, with the applied linear-regression analysis on the experimental points. We can clearly see that there is a more than satisfactory quality of the linear fit, where all points lie within 95 % confidence limits (Fig. 7), and where detected (*not much*) curvature does not affect the subsequent calculated values of the kinetic parameters (A and E_a). From presented results, we may conclude that 0.75 is the most appropriate value for n^* kinetic parameter, and that the detected curvature in Fig. 6 is fundamental. However, this phenomenon can be eventually attributed to the change in the fundamental

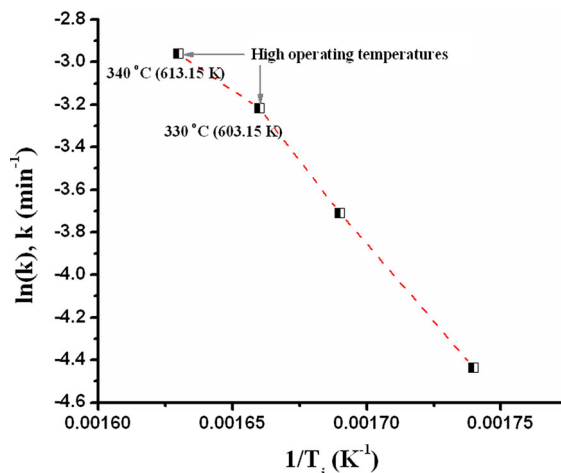


Fig. 6 The dependence of $\ln(k)$ versus $1/T_i$ for the values of k which correspond to the selected apparent reaction order ($n^* = 0.75$) (results for k from Table 5). In the current figure, only the roughly dependence, without establishing a linear-regression analysis to a given experimental points was shown

nature of the reaction. Meanwhile, such curvature (Fig. 6) is an expected outcome of the temperature-induced transition from an energy—to a time-dependent realm, but the goal of this paper is not to check the assumptions outlined above.

On the other hand, we can also see that in the current case, we get a very realistic values of the kinetic parameters [$A = 1.357 \times 10^8$ min⁻¹ and $E_a = 110.4$ kJ mol⁻¹ (Fig. 7)], where all the errors

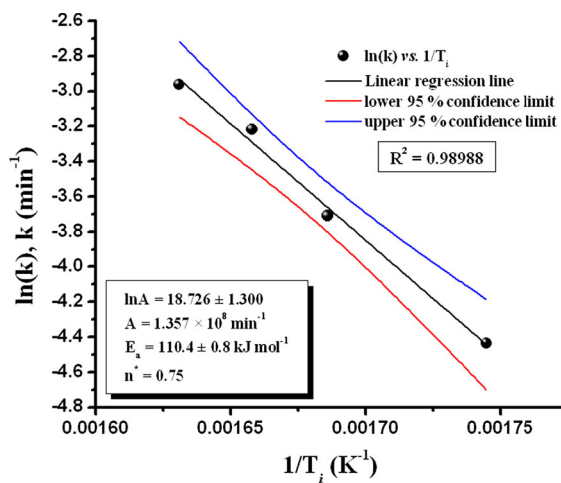


Fig. 7 The Arrhenius plot of $\ln(k)$ versus $1/T_i$, with the applied linear-regression analysis on the experimental points. The corresponding 95 % confidence limits, with lower and upper bounds are clearly marked

meet the expected condition of their entry into the range of the experimental errors. If we compare this value of E_a which was obtained using the procedure presented in Fig. 7, with the value of E_a calculated by the Friedman's isoconversional method ($110.7 \text{ kJ mol}^{-1}$), we can notice almost perfect agreement between them. This means that the average value of E_a calculated using the isoconversional approach is not the "lumped" kinetic parameter, so in the observed α 's, the pyrolysis process of the powdered cellulose can be described through the single-step reaction model.

Using the obtained values of kinetic parameters ($A = 1.357 \times 10^8 \text{ min}^{-1}$; $E_a = 110.4 \text{ kJ mol}^{-1}$) we performed a corresponding numerical calculations of the conversion ($\alpha - t$) curves, based on the relation $\alpha(t) = 1 - [A \cdot \exp(-E_a/RT_i) \cdot t \cdot (n^* - 1) + 1]^{1/(1-n^*)}$, which is valid for $n^* \neq 1$. For all calculations, the apparent reaction order of $n^* = 0.75$ was used.

Figure 8 shows the comparison between the experimentally obtained and calculated (taking into account the relation $\alpha(t) = 1 - [A \cdot \exp(-E_a/RT_i) \cdot t \cdot (n^* - 1) + 1]^{1/(1-n^*)}$ for $n^* = 0.75$) conversion ($\alpha - t$) curves, for the pyrolysis process of the powdered cellulose at the different operating temperatures (300, 320, 330 and 340 °C).

Comparing the experimental and calculated conversion [$\alpha(t)$] curves at all operating temperatures where the pyrolysis process developing (Fig. 8), we can conclude that the isothermal pyrolysis of the powdered cellulose unequivocally follows the reaction mechanism which obeys to non-integer kinetics ($n^* \neq 1$).

However, in order to test accuracy and precision of certain kinetic parameters using classical kinetic approach, the Bayesian inference framework was used.

Discussion of the results obtained from Bayesian inference

Based on the obtained isoconversional dependence estimated using the Vyazovkin's modified non-linear isoconversional approach (Fig. 5), we can calculate the experimental distribution function of E_a values, resulting from $\alpha = \alpha(E_{a,x})$ dependence and the procedure of differentiation, such as $d\alpha(E_{a,x})/dE_{a,x}$. By using this procedure, we obtained the experimental (the initial form of $f(\varepsilon_a; \theta)$, with unknown θ)

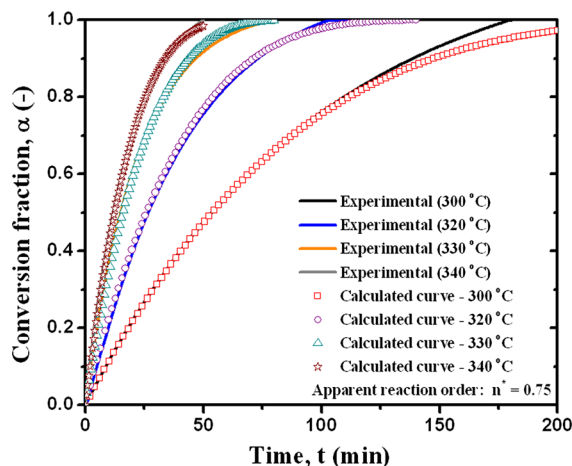


Fig. 8 The comparison between the experimentally obtained and calculated (taking into account the relation $\alpha(t) = 1 - [A \cdot \exp(-E_a/RT_i) \cdot t \cdot (n^* - 1) + 1]^{1/(1-n^*)}$ for $n^* = 0.75$) conversion ($\alpha - t$) curves, for the pyrolysis process of the powdered cellulose at the different operating temperatures (300, 320, 330 and 340 °C)

distribution of E_a values. The shape of the estimated curve is presented in Fig. 9.

We can notice that the experimental distribution function for powdered cellulose pyrolysis process is characterized by single-peak $f(\varepsilon_a; \theta)$ curve (Fig. 9). By using a flexible fitting procedure (OriginLab 2014), it was found that $f(\varepsilon_a; \theta)$ curve is most closely corresponds to the Normal (Gauss) distribution function. The peak of the current curve corresponds to the value of the apparent activation energy equal to $E_{a(\text{peak})} = 106.8 \text{ kJ mol}^{-1}$ (Fig. 9). From Fig. 9, we can see that the E_a values around the peak at higher $f(\varepsilon_a; \theta)$ values, are distributed almost symmetrically, while at lower $f(\varepsilon_a; \theta)$ values, there is some small asymmetry that pulls toward the lower values of the apparent activation energy. The value of apparent activation energy equal to $106.8 \text{ kJ mol}^{-1}$ corresponds to the later stage of pyrolysis process, but this value is even higher than some of the values reported in the literature, and which are less than 100 kJ mol^{-1} (Table 3). This could be associated to the less volatile matter during the first devolatilisation stage, in which the kinetic parameter was considered. The variations in particle sizes and origin sources of celluloses may have an impact on devolatilisation characteristics (Akinrinola et al. 2014; Balogun et al. 2014). Based on the derived $f(\varepsilon_a; \theta)$, we can apply the Bayesian inference framework, which will includes normal

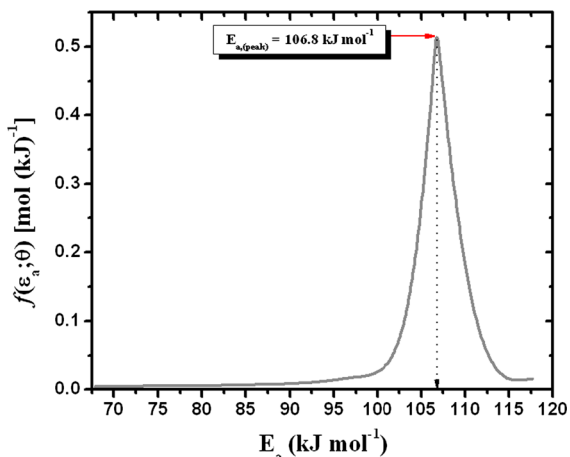


Fig. 9 The experimental density distribution function of E_a values, resulting from $\alpha = \alpha(E_{a,i})$ dependence and the procedure of differentiation throughout $d\alpha(E_{a,i})/dE_{a,i}$, for the isothermal pyrolysis of the powdered cellulose; The peak of the current distribution corresponds to the value of the apparent activation energy equal to $106.8 \text{ kJ mol}^{-1}$

prior and normal posterior estimations, together with searching for unknown parameters, attached to the normal distribution.

Let’s assume that we have a normal population of the apparent activation energy counterparts ($\varepsilon_{a,i}$, with $i = 1, \dots, 100$), with an unknown mean and a known variance. We will take for our analysis, the case with normal likelihood and normal prior combinations, where such a system is the most commonly taken in practice (Lesaffre and Lawson 2012). Assume that an observation $\varepsilon_{a,i} \in E_a$ is normally distributed with mean θ and known variance σ^2 [$\sigma^2 = 1.96 \text{ (kJ mol}^{-1})^2$; $\sigma = 1.4 \text{ kJ mol}^{-1}$]. The parameter of interest, θ , has normal distribution as well with hyperparameters μ and τ^2 . Starting with an Bayesian model of $E_a|\theta \sim \mathcal{N}(\theta, \sigma^2)$ and $\theta \sim \mathcal{N}(\theta, \tau^2)$, we will find the marginal and posterior distributions. The exponent ξ (Iyer et al. 2002) in the joint distribution $h(\varepsilon_a, \theta)$ is:

$$\xi = -\frac{1}{2\sigma^2} (\varepsilon_{a,i} - \theta)^2 - \frac{1}{2\tau} (\theta - \mu)^2. \tag{14}$$

After some mathematical transformations, ξ can be expressed as:

$$\xi = -\frac{1}{2\rho} \left[\theta - \rho \left(\frac{\varepsilon_{a,i}}{\sigma^2} + \frac{\mu}{\tau^2} \right) \right]^2 - \frac{1}{2(\sigma^2 + \tau^2)} (\varepsilon_{a,i} - \mu)^2, \tag{15}$$

where

$$\rho = \frac{\sigma^2 \tau^2}{(\sigma^2 + \tau^2)}. \tag{16}$$

Recall that $h(\varepsilon_a, \theta) = f(\varepsilon_a|\theta) \cdot \pi(\theta) = \pi(\theta|\varepsilon_a) \cdot m(\varepsilon_a)$, so the marginal distribution simply resolves to $E_a \sim \mathcal{N}(\mu, \sigma^2 + \tau^2)$ and posterior distribution becomes:

$$\theta|E_a \sim \mathcal{N} \left(\left(\frac{\tau^2}{(\sigma^2 + \tau^2)} E_a + \frac{\sigma^2}{(\sigma^2 + \tau^2)} \mu, \frac{\sigma^2 \tau^2}{(\sigma^2 + \tau^2)} \right) \right). \tag{17}$$

If $E_{a1}, E_{a2}, \dots, E_{an}$ are observed instead of a single observation E_a , then the sufficiency of \overline{E}_a implies that the Bayesian model for θ is the same as for E_a with σ^2/n ($n = 100$) in place of σ^2 . In other words, the Bayesian model can be expressed as:

$$\overline{E}_a|\theta \sim \mathcal{N} \left(\theta, \frac{\sigma^2}{n} \right), \tag{18}$$

and

$$\theta \sim \mathcal{N}(\mu, \tau^2), \tag{18a}$$

producing

$$\theta|\overline{E}_a \sim \mathcal{N} \left(\left(\frac{\tau^2}{(\frac{\sigma^2}{n} + \tau^2)} \overline{E}_a + \frac{\frac{\sigma^2}{n}}{(\frac{\sigma^2}{n} + \tau^2)} \mu, \frac{\frac{\sigma^2}{n} \tau^2}{(\frac{\sigma^2}{n} + \tau^2)} \right) \right). \tag{19}$$

Then there would be recorded that the posterior mean (μ^*) is equal to

$$\mu^* = \frac{\tau^2}{(\frac{\sigma^2}{n} + \tau^2)} \overline{E}_a + \frac{\frac{\sigma^2}{n}}{(\frac{\sigma^2}{n} + \tau^2)} \mu, \tag{20}$$

which is weighted linear combination of the maximum likelihood estimates (Rohde 2014) \overline{E}_a , and prior mean μ with weights $\lambda = n \cdot \tau^2 / (\sigma^2 + n \cdot \tau^2)$ and $(1 - \lambda) = \sigma^2 / (\sigma^2 + n \cdot \tau^2)$. When the sample size has a tendency to increase, $\lambda \rightarrow 1$, afterwards the influence of the prior mean diminishes. On the other hand, when n is relatively small, and when the prior about μ becomes meaningful (i.e., τ^2 is quite small), in that case, the posterior mean is close to the prior mean μ . From Eq. (20) we can see that a common Bayesian estimator is the posterior mean, while $(\sigma^2/n) \cdot \tau^2 / (\sigma^2/n + \tau^2)$ represents the posterior variance marked with σ^{*2} . In addition, the uncertainty bounds can be found from the

percentiles of posterior distribution. A 95 % credible interval (CI) for θ can be calculated from the relation as:

$$CI = \mu^* \pm 1.96 \cdot \sigma^*, \quad (21)$$

where σ^* is posterior dispersion.

Figure 10 shows the comparison between estimated likelihood function $f(\varepsilon_a|\theta)$ and the experimentally evaluated density distribution function (Fig. 9), for the investigated isothermal pyrolysis process of the powdered cellulose. In addition to the label attached to likelihood function on the black-line inset in Fig. 10, the likelihood function is $\overline{E}_a | \theta \sim \mathcal{N}(\theta, \sigma^2/n = 1.96/100)$; where $\sigma = 1.40 \text{ kJ mol}^{-1}$). The numerical calculations were performed in MATLAB® codes (MATLAB® codes 2014).

We can see that the likelihood function with respect to experimental density function is shifted to the right on the side of higher ε_a counterparts, where $f(\varepsilon_a|\theta)$ unlike to $f(\varepsilon_a; \theta)$ is narrow drastically, so that the placed Bayesian model shows the definition of reliability in E_a values in the direction of slightly higher values of the apparent activation energy in relation to $E_{a(\text{peak})} = 106.8 \text{ kJ mol}^{-1}$, which has been detected in Fig. 9. Also, $f(\varepsilon_a|\theta)$ function in comparison with $f(\varepsilon_a; \theta)$ shows no occurrence of the asymmetry (Fig. 10), which, however, was registered in a small “portions” for the experimental density function (Fig. 9).

Figure 11 shows the estimated prior and posterior distributions, under monitored experimental conditions.

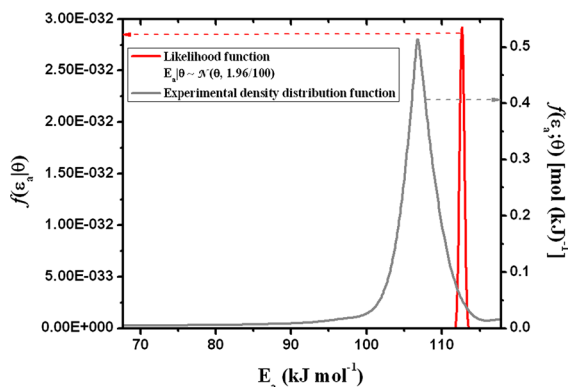


Fig. 10 The comparison between estimated likelihood function $f(\varepsilon_a|\theta)$ and the experimentally evaluated density distribution function (Fig. 9), for the isothermal pyrolysis process of the powdered cellulose

From Fig. 11 we can see that the posterior distribution is almost identical to the model (the likelihood) function, while the prior distribution is positioned at the same location as an experimental density function (Fig. 10), showing a nearly perfect symmetrical shape, compared to $f(\varepsilon_a; \theta)$ function, which was not the case. In fact, prior distribution shows “realistic” shape of experimental distribution of the apparent activation energies, eliminating the appearance of any errors, which would occur during the process of differentiation of $\alpha = \alpha(E_{a,\alpha})$ dependence. This distribution is the inherent characteristics of the pyrolysis process.

Table 6 lists the values of all monitored model parameters, attached to the ingredients of Bayesian inference, which were estimated by the numerical computations.

It can be seen from Table 6 that for our data, the mean of the posterior distribution is a very close to the prior mean. Namely, in the current case, the latter will cause that the dispersion (and therefore variance) of the posterior distribution shrinks (Table 6). This effect is a direct consequence of the real appearance of the posterior distribution, which is shown in Fig. 11. On the other hand, there is 95 % chance that unknown parameter θ is between 112.5 and 113.1 kJ mol^{-1} , and as has been unequivocally confirmed by the results shown in Table 6. The observed θ parameter is in good agreement with the value of E_a ($110.4 \text{ kJ mol}^{-1}$) calculated by logarithmic form of Arrhenius equation (Fig. 7).

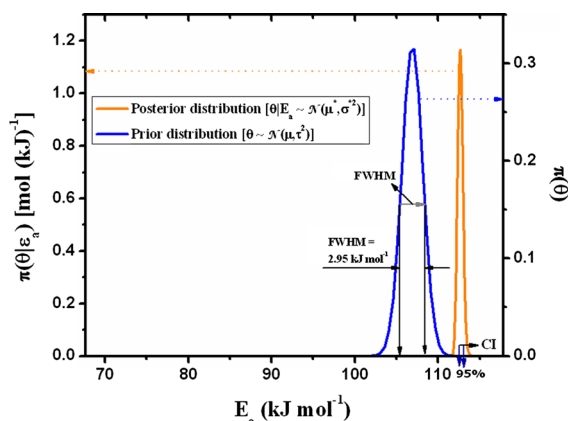


Fig. 11 Estimated prior and posterior distributions whose origins come from the Bayesian inference framework, in the case of pyrolysis process of the powdered cellulose, under isothermal experimental conditions; The full width at half maximum (FWHM) of prior distribution is a clearly marked, where a 95 % credible interval (CI) for θ is also indicated

In Fig. 11, the full width at half maximum (FWHM) of the prior distribution is a clearly marked. The FWHM is a very important feature, and can be associated with the mean of posterior distribution (μ^*) and hyperparameter (τ) through the following equation:

$$\mu^* = c \cdot \frac{FWHM}{\tau}, \quad (22)$$

where μ^* is posterior mean, FWHM is the full width at half maximum attached to the prior distribution [FWHM = 2.95 kJ mol⁻¹ (Fig. 11)], while c represents cellulose characteristic energy constant [kJ mol⁻¹], which can be related with rigidity angle (ψ) as a measure of tenseness of the cellulose chains (2mer, 4mer, 6mer), where $\langle \cos(\psi) \rangle$ is a function of temperature. The last mentioned magnitude exists in the freely rotating chain model (Burchard 1971; Lee et al. 2004; Mazeau and Wyszomirski 2012; Kloczkowski and Kolinski 2007). New term $\langle \cos(\psi) \rangle$ is equal to the magnitude c/RT_i , where R is the gas constant, and T_i is the i th monitored operating temperature.

Table 7 lists the values of c , FWHM and τ which were calculated for the posterior mean, in the considered pyrolysis process of the powdered cellulose samples, under the isothermal conditions.

Value associated with cellulose characteristic energy constant (47.8 kJ mol⁻¹, Table 7) corresponds to formation of pyranoses from the cellulose chain (Włodarczyk 2012), while the value of $\mu^* = 112.8$ kJ mol⁻¹ (Table 6) corresponds to formation of D-fructose (Włodarczyk 2012; Sanders et al. 2002; García Barneto et al. 2011). Furthermore these molecules are involved in the pyrolysis of cellulose,

where clearly follows that the main decomposition reactions start from the cellulose chains, where we can assume that the molecule chain decomposes from both sides to the middle gradually. Hydroxyl (–OH) of inside unit will break earlier than the ring of two-terminals. In addition, from D-fructose structures including additional dehydration steps (Seshadri and Westmoreland 2012), the levoglucosan molecules can be formed.

Assumption that the main decomposition reactions proceed from cellulose chain points, can be confirmed by the change of the values of angle ψ with the increase in operating temperature (T_i), and these results are presented in Table 8.

It can be seen from Table 8 that the value of the angle ψ increases with an increasing of the operating temperature, suggesting that rigidity of cellulose chains decreases and their flexibility are increased. From the above presented results, we can conclude that despite a wide variety of organic components which arises from the pyrolysis process of cellulose, the formation of lower molecular weight products (such as conversion reactions which lead to D-glucose and D-fructose structures) (Luo et al. 2007) plays a significant role in investigated powdered cellulose pyrolysis.

Therefore, we can reasonably assume with a great certainty, that the pyrolysis process of powdered cellulose takes place probably through the formation of levoglucosan, where depolymerization is predominant pathway of breakdown. However, identified six-eighths-order ($n^* = 0.75$) kinetics model may indicates the occurrence of a number of unzipping reactions, which may arise from terminal group of the chain (Belgacem and Gandini 2005). Also, the

Table 6 Values of the model parameters, attached to the ingredients of Bayesian inference, for investigated isothermal pyrolysis of the powdered cellulose samples

Model parameters related to ingredients of Bayesian inference for pyrolysis of the powdered cellulose					
σ (kJ mol ⁻¹) ^a	μ (kJ mol ⁻¹) ^b	τ^2 (kJ mol ⁻¹) ²	CI ^c	θ	
				μ^* (kJ mol ⁻¹) ^d	σ^* (kJ mol ⁻¹) ^e
1.40	112.9	1.56	(112.5, 113.1)	112.8	0.14

^a Known parameter

^b Prior mean

^c Credible interval [in (kJ mol⁻¹)]

^d Posterior mean

^e Posterior dispersion

Table 7 Values of c , FWHM (full width at half maximum at prior) and τ (hyperparameter) calculated for posterior mean (μ^*), for the isothermal pyrolysis of the powdered cellulose

Isothermal pyrolysis of the powdered cellulose		
c (kJ mol ⁻¹)	FWHM (kJ mol ⁻¹)	τ (kJ mol ⁻¹)
47.8	2.95	1.25

appearance of the apparent reaction order less than unity can be due to an increase of the active surface with the reaction extension, so it is possible that in current pyrolysis process, the active surface increases more intensively than in other pyrolysis processes, which have been reported in Table 3 by a variety of researchers, which largely depends on the applied experimental conditions and of initial “form” of cellulose samples. The latter opens the possibility for enactment of radical reactions within the pyrolytic process at higher operating temperatures. The initiation reaction can represent cleavage of C–OH bonds. OH radicals abstract hydrogen atom from a cellulose molecule forming water (which leaves the observed system) and a propagating radical. A successive β -scission can form a double bond inside the polymer chain and release another OH radical, which rapidly propagates the chain. It should be noted that obtained posterior mean (112.8 kJ mol⁻¹, Table 6) exceeds the average value for water-anion hydrogen bond strength (about 52.0 kJ mol⁻¹) as the isolated system in the gas phase.

In addition to the above-mentioned pathway, the second pathway probably represents the decomposition or fragmentation in which the cellulose ring opens up and breaks down into two or three carbon oxygenated compounds. In this case, we can expect that the predominant products are hydroxyacetaldehyde, formaldehyde, acetol, methyl glyoxal and

Table 8 Changes in the value of the angle ψ [angle is given in radians (rad) and in degrees (°)], with the increase of operating temperature (T_i) during the isothermal pyrolysis of the powdered cellulose

T_i (°C)	$\langle \cos(\psi) \rangle$	ψ (rad)	ψ (°)
300	10.03112	-0.82174	0.98471
320	9.69289	-0.96427	0.98572
330	9.53219	-0.99424	0.98619
340	9.37672	-0.99885	0.98665

glyoxal (Chundawat et al. 2011; Zhang et al. 2014; Lédé 2012).

It should be noted that at higher operating temperatures (beyond 300 °C), the depolymerization of the cellulose chain and formation of anhydroglucose derivatives, volatile organic materials and tars can probably be achieved in observed experimental conditions.

However, it should be noted that low molecular weight compounds, including glycolaldehyde, could be produced from the cellulose pyrolysis under the conditions of the minimal levoglucosan degradation, which may suggest the existence of competitive nature of the primary pyrolysis reactions (Lédé 2012). This just may be assumed, if we take into account the resulting range of ε_a counterparts and value of FWHM (Fig. 11; Table 7).

It should be noted that the kinetic treatment of pyrolytic behavior of cellulose in wood biomass (as in the softwood and hardwood species) systems (Janković 2014) and as an isolated reaction system (considered over Bayesian statistics procedure) is obviously not the same, and shows significantly different results, related to different kinetics ascribed to the cellulose decompositions. Also, it should be noted that the volatilization rate is more temperature-sensitive, i.e., has the higher apparent activation energy, than the charring rate (Williams and Besler 1996).

Bayesian statistical approach provides a much “clearer” picture of the cellulose pyrolytic process as an isolated reaction system, than in the case when the pyrolysis of cellulose is considered in the context of the thermal degradation of biomass (Janković 2014), which is a much more complex reaction system, and that takes into account all possible decomposition reactions arising from three main pseudo-components (cellulose, hemicelluloses and lignin).

Conclusions

Bayesian inference was used to test the powdered cellulose pyrolysis, under the isothermal (static) experimental conditions. In general, this approach was firstly applied in the kinetic treatment of the pyrolysis process for lignocellulosic materials. A completely new procedure that was based on obtaining the reliable distribution functions of effective activation energy

(E_a) values by the statistical derivation of prior and posterior functions was introduced. It should be noted that as an important conclusion justified in the current paper was as follows: the kinetic treatment of pyrolytic behavior of cellulose in wood biomass (such as softwood and hardwood species) (compared to the earlier reported results) and as an isolated (independent) molecular system using the Bayesian inference framework, is obviously not the same and shows significantly different results related to the different kinetics of cellulose decomposition reactions.

It has been found that the pyrolysis of the powdered cellulose can be described by the kinetics, which differs from the first-order model. Also, it was established that the apparent activation energy value presented as the average magnitude in the conversion fraction range of $0.20 \leq \alpha \leq 0.65$ does not represent “lumped” kinetic parameter, so in indicated α 's range, the pyrolysis process can be described through the single-step reaction model with six-eighths-order ($n^* = 0.75$) kinetics. Based on the presented Bayesian inference results, it was assumed that the mechanism of pyrolysis takes place through the decomposition reactions which start from the cellulose chains.

On the basis of the discussed mechanism, and perceived characteristics of prior and posterior distributions, it was found that the pyrolysis process of powdered cellulose takes place probably through the formation of levoglucosan, where depolymerization is predominant reaction pathway.

Acknowledgments This research work was partially supported by the Ministry of Science and Environmental Protection of Serbia under project No. 172015.

References

- Agrawal R (1988a) Kinetics of reactions involved in pyrolysis of cellulose I. The three reaction model. *Can J Chem Eng* 66:403–412
- Agrawal R (1988b) Kinetic of reactions involved in pyrolysis of cellulose II. The modified Kilzer-Broido model. *Can J Chem Eng* 66:413–418
- Akinrinola FS, Darvell LI, Jones JM, Williams A, Fuwape JA (2014) Characterization of selected Nigerian biomass for combustion and pyrolysis applications. *Energy Fuels* 28:3821–3832
- Aldrich J (1997) RA Fisher and the making of maximum likelihood 1912–1922. *Stat Sci* 12:162–176
- Antal M, Varhegyi G (1995) Cellulose pyrolysis kinetics: the current state of knowledge. *Ind Eng Chem Res* 34:703–717
- Arora S, Lal S, Kumar S, Kumar M, Kumar M (2011) Comparative degradation kinetic studies on three biopolymers: chitin, chitosan and cellulose. *Arch Appl Sci Res* 3:188–201
- Aven T, Kvaløy JT (2002) Implementing the Bayesian paradigm in risk analysis. *Reliab Eng Sys Saf* 78:195–201
- Balogun AO, Lasode OA, McDonald AG (2014) Thermo-analytical and physico-chemical characterization of woody and non-woody biomass from an agro-ecological zone in Nigeria. *Bioresources* 9:5099–5113
- Bamford CH, Tipper CFH (1980) Comprehensive Chemical kinetics. In: Bamford CH, Tipper CFH (eds.) Vol. 22, Elsevier, Amsterdam
- Belgacem MN, Gandini A (2005) Surface modification of cellulose fibres. *Polímeros: Ciência e Tecnologia* 15:114–121
- Bigger S, Scheirs J, Camino G (1998) An investigation of the kinetics of cellulose degradation under non-isothermal conditions. *Polym Degrad Stab* 62:33–40
- Blasi C (1994) Numerical simulation of cellulose pyrolysis. *Biomass Bioenerg* 7:87–98
- Bradbury A, Sakai Y, Shafizadeh F (1979) Kinetic model for pyrolysis of cellulose. *J Appl Polym Sci* 23:3271–3280
- Burchard W (1971) Statistics of stiff chain molecules: III. Chain length dependence of the mean square radius of gyration of cellulose- and amylose-tricarbanilates. *British Polym J* 3:214–221
- Cabrales L, Abidi N (2010) On the thermal degradation of cellulose in cotton fibers. *J Therm Anal Calorim* 102:485–491
- Capart R, Khezami L, Burnham AK (2004) Assessment of various kinetic models for the pyrolysis of a microgranular cellulose. *Thermochim Acta* 417:79–89
- Chen WH, Kuo PC (2011) Isothermal torrefaction kinetics of hemicellulose, cellulose, lignin and xylan using thermogravimetric analysis. *Energy* 36:6451–6460
- Chundawat SPS, Beckham GT, Himmel ME, Dale BE (2011) Deconstruction of lignocellulosic biomass to fuels and chemicals. *Ann Rev Chem Biomol Eng* 2:121–145
- Conesa J, Caballero J, Marcilla A, Font R (1995) Analysis of different kinetic models in the dynamic pyrolysis of cello. *Thermochim Acta* 254:175–192
- Diebold J (1994) A unified, global model for the pyrolysis of cellulose. *Biomass Bioenerg* 7:75–85
- Ding HZ, Wang ZD (2008) On the degradation evolution equations of cellulose. *Cellulose* 15:205–224
- Emsley AM, Stevens GC (1994) Kinetics and mechanisms of the low-temperature degradation of cellulose. *Cellulose* 1:26–56
- Eom Y, Kim S, Kim SS, Chung SH (2006) Application of peak property method for estimating apparent kinetic parameters of cellulose pyrolysis reaction. *J Ind Eng Chem* 12:846–852
- Flynn JH (1997) The ‘temperature integral’—its use and abuse. *Thermochim Acta* 300(1–2):83–92
- Friedman HL (1963) Kinetics of thermal degradation of charfoaming plastics from thermogravimetry—application to a phenolic resin. *Polym Sci C* 6:183–195
- García Barneto A, Vila C, Ariza J, Vidal T (2011) Thermogravimetric measurement of amorphous cellulose content in flax fibre and flax pulp. *Cellulose* 18:17–31

- Grønli M, Antal M, Varhegyi GX (1999) Round-robin study of cellulose pyrolysis kinetics by thermogravimetry. *Ind Eng Chem Res* 38:2238–2244
- Hedwall JA (1938) *Reaktionsfähigkeit Festen Stoffe*, Barth JA: Leipzig
- Iyer SK, Manjunath D, Manivasakan R (2002) Bivariate exponential distributions using linear structures. *Sank Indian J Stat* 64:156–166
- Janković B (2014) The pyrolysis process of wood biomass samples under isothermal experimental conditions—energy density considerations: application of the distributed apparent activation energy model with a mixture of distribution functions. *Cellulose* 21:2285–2314
- Jovanović R (1989) Edition: the science of fiber and fiber technology. II. Cellulose natural and chemical fibers. Building Book Press, University of Belgrade, Belgrade, pp 112–118
- Karabatsos G, Walker SG (2006) On the normalized maximum likelihood and Bayesian decision theory. *J Math Psychol* 50:517–520
- Khachani M, El Hamidi A, Halim M, Arsalane S (2014) Non-isothermal kinetic and thermodynamic studies of the dehydroxylation process of synthetic calcium hydroxide $\text{Ca}(\text{OH})_2$. *J Mater Environ Sci* 5:615–624
- Khawam A, Flanagan DR (2006) Solid-state kinetic models: basics and mathematical fundamentals. *J Phys Chem B* 110:17315–17328
- Kim S, Eom Y (2006) Estimation of kinetic triplet of cellulose pyrolysis reaction from isothermal kinetic results. *Korean J Chem Eng* 23:409–414
- Kloczkowski A, Kolinski A (2007) Theoretical models and simulations of polymer chains. In: Mark JE (ed) *Physical properties of polymers handbook*. Springer Science + Business Media, New York, pp 67–83
- Langston PA, Burbidge AS, Jones TF, Simmons MJH (2001) Particle and droplet size analysis from chord measurements using Bayes theorem. *Powder Technol* 116:33–42
- Lédé J (2012) Cellulose pyrolysis kinetics: an historical review on the existence and role of intermediate active cellulose. *J Anal Appl Pyrol* 94:17–32
- Lee PM (2012) *Bayesian statistics: an introduction*, 4th edn. Wiley, London, pp 36–77
- Lee G, Nowak W, Jaroniec J, Zhang Q, Marszalek PE (2004) Molecular dynamics simulations of forced conformational transitions in 1,6-linked polysaccharides. *Biophys J* 87:1456–1465
- Lesaffre E, Lawson A (2012) *Bayesian biostatistics—statistics in practice*, part I. Basic concepts in Bayesian methods. Wiley, London, pp 106–114
- Lester E, Watts D, Cloke M, Langston P (2003) Determining the composition of binary cial blends using Bayes theorem. *Fuel* 82:117–125
- Liao YF, Wang SR, Ma XQ (2004) Study of reaction mechanisms in cellulose pyrolysis. *Prepr Pap Am Chem Soc Div Fuel Chem* 49(1):407–411
- Liau LCK, Hsieh YP (2005) Kinetic analysis of poly(vinyl butyral)/glass ceramic thermal degradation using non-linear heating functions. *Polym Degrad Stab* 89:545–552
- Liu Z, Jiang Z, Fei B, Liu X (2013) Thermal decomposition characteristics of Chinese fir. *Bioresources* 8:5014–5024
- Luo N, Cao F, Zhao X, Xiao T, Fang D (2007) Thermodynamic analysis of aqueous-reforming of polyols for hydrogen generation. *Fuel* 86:1727–1736
- Martz H, Waller R (1985) *Bayesian reliability analysis*. Wiley, New York, pp 35–45
- MATLAB[®] codes, <http://www.mathworks.com/products/matlab/examples.html>, 2014
- Mayo DG (2010) An error in the argument from conditionality and sufficiency to the likelihood principle. In: Mayo DG, Spanos A (eds) *Error and inference—recent exchanges on experimental reasoning, reliability and the objectivity and rationality of science*. Cambridge University Press, Cambridge, pp 305–314
- Mazeau K, Wyszomirski M (2012) Modelling of Congo red adsorption on the hydrophobic surface of cellulose using molecular dynamics. *Cellulose* 19:1495–1506
- Mettler MS, Mushrif SH, Paulsen AD, Javadekar AD, Vlachos DG, Dauenhauer PJ (2012) Revealing pyrolysis chemistry for biofuels production: conversion of cellulose to furans and small oxygenates. *Energy Environ Sci* 5:5414–5424
- Milne TA, Brennan AH, Glenn BH (1990) *Sourcebook of methods of analysis for biomass and biomass conversion processes*. Elsevier, London, pp 51–67
- Mui ELK, Cheung WH, Lee VKC, McKay G (2010) Compensation effect during the pyrolysis of tyres and bamboo. *Waste Manag* 30:821–830
- Muller-Hagedorn M, Bockhorn H, Krebs L, Muller U (2003) A comparative kinetic study on the pyrolysis of three different wood species. *J Anal Appl Pyrol* 68–69:231–249
- Myung JI, Navarro DJ, Pitt MA (2006) Model selection by normalized maximum likelihood. *J Math Psychol* 50:167–179
- OriginLab Tutorial, The nonlinear curve fitter (NLFit) (2014) using the origin's fitting function builder. ©OriginLab Corporation, <http://www.originlab.com>
- Poletto M, Pistor V, Santana RMC, José Zattera A (2012) Materials produced from plant biomass. Part II: evaluation of crystallinity and degradation kinetics of cellulose. *Mater Res* 15:421–427
- Robert C (2001) *The Bayesian choice: from decision-theoretic motivations to computational implementation*, 2nd edn. Springer, New York, pp 38–43
- Rohde CA (2014) Introductory statistical inference with the likelihood function, Chapter 14. *Bayesian inference*. Springer, New York, pp 167–181. ISBN 978-3-319-10460-7
- Royall R (1997) *Statistical evidence: a likelihood paradigm*. Chapman & Hall/CRC, New York, pp 1–31
- Sánchez-Jiménez PE, Pérez-Maqueda LA, Perejón A, Pascual-Cosp J, Benítez-Guerrero M, Criado JM (2011) An improved model for the kinetic description of the thermal degradation of cellulose. *Cellulose* 18:1487–1498
- Sánchez-Jiménez PE, Pérez-Maqueda LA, Perejón A, Criado JM (2013) Generalized master plots as a straightforward approach for determining the kinetic model: the case of cellulose pyrolysis. *Thermochim Acta* 552:54–59
- Sanders EB, Goldsmith AI, Seeman JI (2002) A model that distinguishes the pyrolysis of D-glucose, D-fructose, and sucrose from that of cellulose. Application to the understanding of cigarette smoke formation. *J Anal Appl Pyrol* 66:29–50

- Seshadri V, Westmoreland PR (2012) Concerted reactions and mechanism of glucose pyrolysis and implications for cellulose kinetics. *J Phys Chem A* 116:11997–12013
- Shaik SM, Koh CY, Nicholas Sharratt P, Tan Reginald BH (2013) Influence of acids and alkalis on transglycosylation and β -elimination pathway kinetics during cellulose pyrolysis. *Thermochim Acta* 566:1–9
- Sonobe T, Worasuwannarak N (2008) Kinetic analyses of biomass pyrolysis using the distributed activation energy model. *Fuel* 87:414–421
- Tang J, Zhuang Q (2009) A global sensitivity analysis and Bayesian inference framework for improving the parameter estimation and prediction of a process-based Terrestrial Ecosystem Model. *J Geophys Res* 114:D15303–D15322
- Varhegyi G, Antal M (1989) Kinetics of the thermal decomposition of cellulose, hemicellulose, and sugar cane bagasse. *Energy Fuels* 3:329–335
- Vyazovkin S (1996) A unified approach to kinetic processing of nonisothermal data. *Int J Chem Kinet* 28:95–101
- Vyazovkin S (1997a) Advanced isoconversional method. *J Therm Anal Calorim* 49:1493–1499
- Vyazovkin S (1997b) Evaluation of activation energy of thermally stimulated solid-state reactions under arbitrary variation of temperature. *J Comput Chem* 18(3):393–402
- Vyazovkin S (2001) Modification of the integral isoconversional method to account for variation in the activation energy. *J Comput Chem* 22(2):178–183
- Vyazovkin S, Wight CA (1997) Isothermal and nonisothermal reaction kinetics in solids: in search of ways toward consensus. *J Phys Chem A* 101:8279–8284
- Vyazovkin S, Wight CA (1999) Model-free and model-fitting approaches to kinetic analysis of isothermal and nonisothermal data. *Thermochim Acta* 340–341:53–68
- Williams PT, Besler S (1996) The influence of temperature and heating rate on the pyrolysis of biomass. *Renew Energy* 7:233–250
- Włodarczyk P (2012) Experimental and theoretical studies on mutarotation in supercooled liquid state. PhD Thesis (A thesis submitted for the degree of Philosophiae Doctor), Prof. Paluch, M., Institute of Physics, Uniwersytecka 4, 40-008 Katowice, University of Silesia, Poland, 2012, pp. 63–68
- Yang H, Yan R, Chin T, Tee DL, Chen H, Zheng C (2004) Thermogravimetric analysis—fourier transform infrared analysis of palm oil waste pyrolysis. *Energy Fuels* 18:1814–1821
- Zhang Y, Liu C, Xie H (2014) Mechanism studies on β -D-glucopyranose pyrolysis by density functional theory methods. *J Anal Appl Pyrol* 105:23–34